

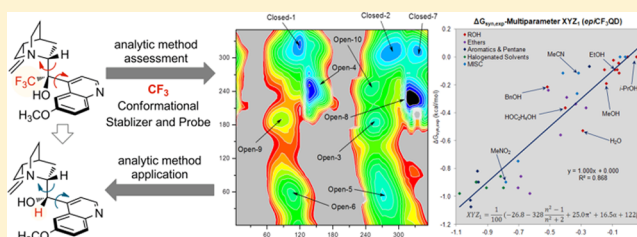
The Trifluoromethyl Group as a Conformational Stabilizer and Probe: Conformational Analysis of Cinchona Alkaloid Scaffolds

G. K. Surya Prakash,* Fang Wang, Martin Rahm, Zhe Zhang, Chuanfa Ni, Jingguo Shen, and George A. Olah

Loker Hydrocarbon Research Institute, Department of Chemistry, University of Southern California, Los Angeles, California 90089, United States

S Supporting Information

ABSTRACT: The introduction of the CF₃ group on the C9 atom in quinidine can significantly increase the conformational interconversion barrier of the cinchona alkaloid scaffold. With this modification the conformational behavior of cinchona alkaloids in various solvents can be conveniently investigated via ¹⁹F NMR spectroscopy. Based on the reliable conformational distribution information obtained, the accuracy of both theoretical (PCM) and empirical (Kamlet–Taft) solvation models has been assessed using linear free energy relationship methods. The empirical solvation model was found to provide accurate prediction of solvent effects, while PCM demonstrated a relatively low reliability in the present study. Utilizing similar empirical solvation models along with Karplus-type equations, the conformational behavior of quinidine and 9-*epi*-quinidine has also been investigated. A model S_N2 reaction has been presented to reveal the important role of solvent-induced conformational behavior of cinchona alkaloids in their reactivity.



1. INTRODUCTION

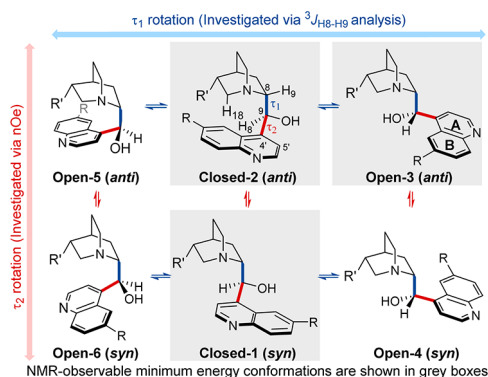
Cinchona alkaloid-based catalysts are privileged chiral scaffolds in asymmetric catalysis.¹ In an effort to improve their catalytic efficacy, in-depth mechanistic insight has been ardently sought. Among various factors, the conformations of catalysts have long been proposed to play a pivotal role in cinchona alkaloid-based catalysis.² Although this hypothesis has been invoked by both experiments^{3–7} and theory,⁸ the conformational behavior of cinchona alkaloids is still not thoroughly understood due to its capricious nature.

Pioneering studies by Dijkstra, Wynberg, and Sharpless have shown that the substantial fluxionality of cinchona alkaloids arises from rotations around the C8–C9 and C4′–C9 bonds (τ_1 and τ_2 , respectively, Scheme 1).³ The τ_1 rotation leads to the interconversion of closed and open conformations, in which the quinuclidine nitrogen points to and away from ring A of quinoline, respectively. Through the τ_2 rotation, *syn* and *anti* conformations are generated, as differentiated by the relative orientation of the –OH group aligning along and apart from ring B of the quinoline moiety, respectively.

Detailed studies by Baiker,^{5,9} Zeara,¹⁰ and others^{7a,11} have revealed that the conformational behavior of cinchona alkaloids could be significantly influenced by various intermolecular forces, such as dipole–dipole interactions, hydrogen-bonding interactions, and protonation on the quinuclidine nitrogen. Due to the complicated conformational scenario, multiple techniques are required for conformational studies of cinchona alkaloids.

Among various means, quantum chemical calculations have been extensively used to provide precise descriptions of three-

Scheme 1. Six Possible Conformations of Cinchona Alkaloids Generated via Rotations around τ_1 and τ_2



dimensional structures of conformers. Three predominant minimum energy species have been identified in the gas phase, namely open-3, closed-1, and closed-2 conformers (Scheme 1).^{3,12} Energy calculations of conformers in solution are usually performed with an implicit consideration of solvent molecules. However, since cinchona alkaloids can interact with solvents via H-bonding, the accuracy of such calculations can be limited.¹³

In comparison, NMR spectroscopic techniques have been widely applied in liquid-phase conformational analyses. Since theoretical studies have found that conformers closed-1 and

Received: May 1, 2014

Published: June 30, 2014

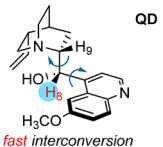

closed-2 are very similar in $\varphi_{\text{H8C9C8H9}}$ dihedral angles,⁵ closed-1 and closed-2 conformations are expected to have practically the same $^3J_{\text{H8H9}}$ coupling constant.¹⁴ Hence, the open–closed equilibrium can be quantified via the $^3J_{\text{H8H9}}$ coupling analysis using the following two-equation, two-variable system,⁵

$$J_{\text{H8H9}}^{\text{obs}} = J_{\text{H8H9}}^{\text{open-3}} \times \text{Pop}_{\text{open-3}} + J_{\text{H8H9}}^{\text{closed}} \times \text{Pop}_{\text{closed}} \quad (1)$$

$$\text{Pop}_{\text{open-3}} + \text{Pop}_{\text{closed}} = 100\% \quad (2)$$

wherein $J_{\text{H8H9}}^{\text{obs}}$ is the observed J_{H8H9} , and $J_{\text{H8H9}}^{\text{open-3}}$ and $J_{\text{H8H9}}^{\text{closed}}$ are J_{H8H9} of open-3 conformation and closed conformations, respectively. $\text{Pop}_{\text{open-3}}$ and $\text{Pop}_{\text{closed}}$ are the populations of open-3 conformation and closed conformations, respectively. Since the conformational equilibrium was indirectly determined on the basis of Karplus-type correlations¹⁴ with the exclusion of minor conformers, systematic errors are expected (Scheme 2).

Scheme 2. Comparison of Conventional Cinchona Alkaloid Conformational Analysis and the Present Trifluoromethyl Conformational Stabilizing/Probing Strategy

Conventional Analysis	Analytical Tools	Possible errors/Problems
 <p>QD fast interconversion</p>	¹ H NMR	deuterated solvents required
	Karplus-type equations	exclusion of minor conformers; accuracy of Karplus correlation
	nOe spectroscopy	semi-quantitative
	theoretical calculations	accuracy of solvation model
CF ₃ -Facilitated Analysis	Analytical Tools	Possible errors/Advantages
 <p>epi-CF₃QD slow interconversion</p>	the CF ₃ group	increase steric hindrance around C9 atom; weakly coordinating
	¹⁹ F NMR	applicable in most solvents; direct measurement of conformational distribution
	nOe spectroscopy	only employed for qualitative conformational analysis
	theoretical calculations	accuracy can be assessed based on ¹⁹ F NMR data

In contrast to the relatively well studied τ_1 rotation, the τ_2 rotation has been rarely explored due to the absence of the corresponding vicinal protons. Even though nuclear Overhauser enhancement (NOE) spectroscopy can deliver information on τ_2 qualitatively, its accuracy in the quantification of conformational equilibria is under debate (Scheme 2).¹⁵ In practice, systematic conformational studies on cinchona alkaloids have also been obstructed by the availability of deuterated solvents, which are necessary in most of the above-mentioned NMR experiments (Scheme 2). The conformational study of cinchona alkaloids in liquid media has thus remained a challenge because of (a) the difficulty in obtaining accurate experimental conformational distribution data, (b) the limited reliability of quantum chemical calculations, and (c) the lack of coherent studies of solvent effects on the conformational behavior of cinchona alkaloids.

Addressing such inherent challenges, we recently demonstrated that the sterically bulky CF₃ group¹⁶ could be incorporated into the C9 atom in quinidine as a conformational stabilizer and a probe (Scheme 2).¹⁷ The mechanistic basis underlying this protocol is the significantly increased barrier to the τ_2 rotation, which leads to the decoalescence of the signals of the *syn* and the *anti* conformations in both ¹H and ¹⁹F NMR spectra at room temperature. The determination of the corresponding conformational equilibria is thus enabled by ¹⁹F NMR peak integration.¹⁸ This direct analytical protocol is not only more precise than the vicinal coupling constant

analysis or 2D NOE spectroscopy, but also applicable in both deuterated and non-deuterated solvents (Scheme 2). With this protocol, a more diverse selection of solvents could be applied for a systematic investigation of solvent effects. Based on the accurate conformational information thus obtained, possible errors in relative energy calculations can be assessed (Scheme 2). Since H-bonding moieties (the hydroxyl and the amino groups) remain intact in the trifluoromethylated analogue (*epi*-CF₃QD), various specific solvent–solute interactions are expected to be relatively unperturbed. More importantly, due to its weakly interacting nature, the CF₃ group, although bulky, should only introduce negligible specific interactions to solvents. Thus, the environmental dependence of the conformations of *epi*-CF₃QD is anticipated to largely reflect that of naturally occurring cinchona alkaloids, and the conformational behavior of the latter can be investigated using a similar protocol. Based on the above-mentioned method, reliable cinchona alkaloid conformational distributions in solution can be obtained, which are informative for the elucidation of active conformations in chemical reactions.

In this article, we quantitatively analyze the solvent dependence of the conformational behavior of cinchona alkaloids, which is primarily facilitated by a combination of NMR studies and density functional theory (DFT) calculations. Initially, we performed the DFT calculations on quinidine (QD) and its derivatives. In the Results and Discussion, section 3.1 addresses DFT calculations of the geometry of conformers of cinchona alkaloids and their derivatives, such as *epi*-CF₃QD, QD and 9-*epi*-quinidine (*epi*-QD); (b) DFT calculations of the relative energies of these conformers and the corresponding conformational distribution in the gas phase and in solution. The second section focuses on the quantitative assessment of the reliability of quantum chemical calculation based on the accurate conformational information on *epi*-CF₃QD obtained from ¹⁹F NMR spectroscopy. Section 3.2 describes determination of the *syn*–*anti* conformational distribution of *epi*-CF₃QD in various solvents via ¹⁹F NMR spectroscopy (3.2.1), systematic analysis of solvent effects on *epi*-CF₃QD conformational behavior based on linear free energy relationship (LFER) (3.2.2), and assessment of the accuracy of the quantum chemical calculation by comparing calculated conformational distribution of *epi*-CF₃QD with experimental outcomes (3.2.3). This section leads to the conclusion that the small solvation energy difference of conformers cannot be adequately predicted by implicit solvation models, such as the polarizable continuum model (PCM) commonly used in cinchona alkaloid conformational studies. This is primarily due to the inaccurate description of specific solvent–solute interactions by the PCM.

In section 3.3, we discuss the solvent-dependent conformational behavior of *epi*-QD. This section involves determination of the open–closed conformational distribution of *epi*-QD in various solvents via ¹H NMR spectroscopy and Karplus-type analysis, analysis of solvent effects on *epi*-QD conformational behavior based on LFER, and assessment of quantum chemical calculations based on experimental data, which demonstrates that conformers with >3.5 kcal/mol relative energies in the gas phase are unlikely to be populated in solution.

Section 3.4 deals with the determination of the open–closed conformational distribution of QD in solution via ¹H NMR spectroscopy and Karplus-type analysis, systematic analysis of solvent effects on QD conformational behavior based on LFER, and quantitative evaluation of the calculated conformational

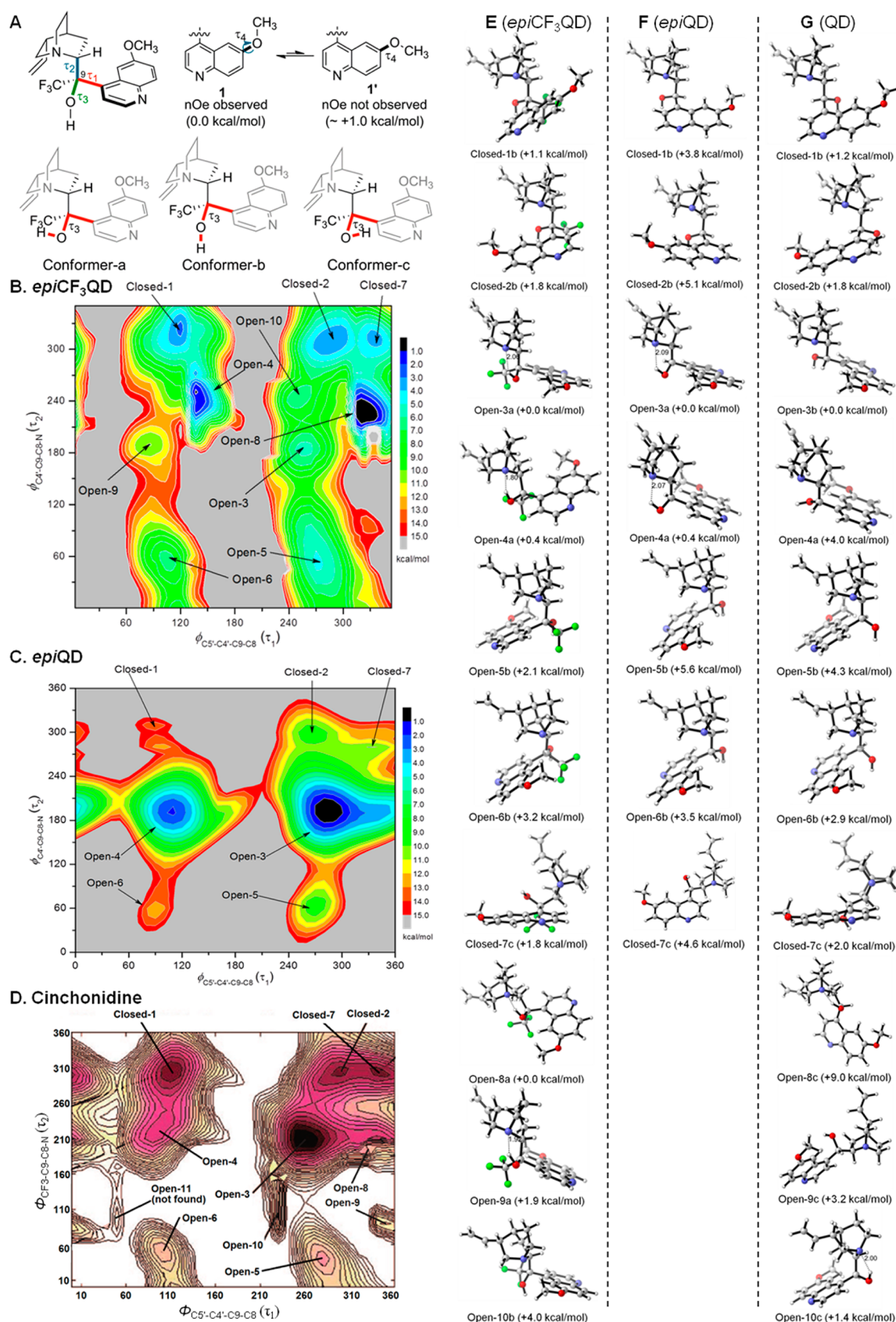


Figure 1. (A) Critical rotations considered in conformational analysis. (B–D) PESs of *epi*-CF₃QD, *epi*-QD, and cinchonidine^{9d} in the gas phase, respectively. (E–G) Representative conformers of *epi*-CF₃QD, *epi*-QD, and QD in the gas phase, respectively; relative Gibbs free energies (gas phase) are shown in parentheses. Panel D is reprinted with permission from ref 9d. Copyright 2008 American Chemical Society.

behavior of QD in solution, showing that PCM may not be suitable for conformational study of QD.

In section 4, a case study demonstrates that the reactivity of QD in a model S_N2 reaction can be significantly affected by solvent-induced conformation changes, implying a pivotal role for conformational behavior of cinchona alkaloids in related reactions.

2. METHODS

2.1. Identification of Conformers via DFT Calculations. The conformations of cinchona alkaloid scaffolds are primarily determined by two critical rotations, τ_1 and τ_2 (Figure 1A). To identify the major conformations of a given cinchona alkaloid derivative, a potential energy surface (PES) as a function of τ_1 and τ_2 was calculated at the B3LYP/6-31+G(d) level in the gas phase using Gaussian 09.¹⁹ The dihedral angles of the two rotations were systematically varied from 0° to 360° by increments of 10° . The obtained conformations were further optimized over five steps for each constrained dihedral angles.²⁰ The conformational profile was formed as a 36×36 PES with 1296 geometry optimizations, revealing a series of conformations (numbered similarly to the previous report by Baiker, Figure 1B,C).^{9d} Based on these structures, further refinement was performed at the B3LYP/6-311+G(d,p) level in the gas phase, which led to very small geometric changes.

In addition to the τ_1 and the τ_2 rotations, two more rotations, τ_3 and τ_4 , were also taken into consideration as they could result in the formation of intramolecular H-bonding and/or significant change in the dipole moment of conformers. Our theoretical calculations showed that **1'**-like conformers are approximately 1 kcal/mol higher in energy than **1** in the gas phase (Figure 1A). Similar results were obtained in the liquid phase by NOESY spectroscopy, in which only **1**-like conformations were detected. Based on these results, **1'** was not considered for further calculations. As τ_3 has three minima around its rotational axis, the number of possible conformations identified on the PES tripled. The additional conformers due to the τ_3 rotation were also optimized at the B3LYP/6-311+G(d,p) level in the gas phase. Since τ_1 and τ_2 angles were essentially unchanged upon the τ_3 rotation, the conformers generated due to the τ_3 rotation were differentiated by alphabetic appendices (such as closed-1a, closed-1b, and closed-1c, Figure 1A). In other words, for a given molecule, the conformers with the same numerical name have similar τ_1 and τ_2 values (however, for different molecules, the same numerical name may not indicate similar τ_1 and τ_2 values).

2.2. Energy Calculation and Population Distribution. To obtain accurate estimates of each conformer's energy, single-point energies were calculated at the M06-2X/6-311+G(d,p)//B3LYP/6-311+G(d,p) level of theory. The hybrid meta exchange-correlation density functional M06-2X empirically accounts for dispersive interactions and has demonstrated high accuracy in main-group thermochemistry.²¹ Solvent effects were included implicitly through the self-consistent reaction field approach, as implemented in the default PCM model in Gaussian 09.^{22,23} Thermal and entropic corrections for both gas-phase and PCM-optimized structures were obtained by frequency analysis at the B3LYP/6-311+G(d,p) level in the gas phase. The frequency analyses also confirmed that all considered structures were true minima on the PES.

The relative population of each conformer at 298 K was derived using the Boltzmann equation. Herein, $\Delta G_{syn,cal}$ is defined as the free energy corresponding to the difference between the calculated *syn* population relative to the calculated *anti* population,

$$\Delta G_{syn,cal} = -RT \ln \left(\frac{\sum Pop_{syn}}{\sum Pop_{anti}} \right) \quad (3)$$

$\Delta G_{open,cal}$ is similarly defined as

$$\Delta G_{open,cal} = -RT \ln \left(\frac{\sum Pop_{open}}{\sum Pop_{closed}} \right) \quad (4)$$

Intramolecular H-bonding interactions were investigated by second-order perturbation analysis of natural bond orbitals (NBOs).²⁴ The

NBO framework ascribes charge transfer as the major contributor to H-bonding, and enables comparison between relevant quinuclidine- $N \rightarrow \sigma_{O-H}^*$ interaction energies.

2.3. NMR Experiments. The conformational analysis of *epi*-CF₃QD in CDCl₃ and DMSO-*d*₆ was achieved via NOESY and HOESY with a concentration of 15 mM at 298 K, and the corresponding conformational distribution was determined by ¹H NMR and ¹⁹F NMR peak integrations. To determine the *syn*–*anti* conformational distribution of *epi*-CF₃QD in other solvents, we initially focused on the assignment of ¹⁹F NMR signals. In most non-alcoholic solvents, the ¹⁹F NMR signal corresponding to the *syn* conformations appeared downfield to that of the *anti* conformations (Figure 2C,D). In alcohols and water, the ¹⁹F NMR signal of the *syn*

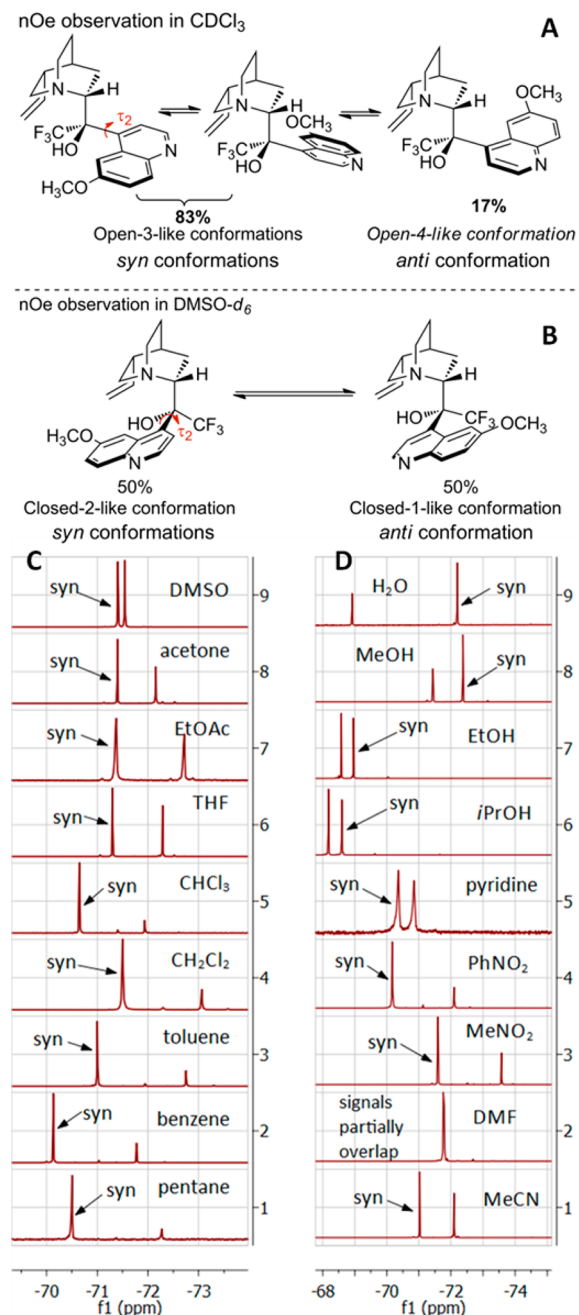


Figure 2. (A) Observed conformational distribution of *epi*-CF₃QD in CDCl₃ (B) Observed conformational distribution of *epi*-CF₃QD in DMSO-*d*₆ (C,D) ¹⁹F NMR spectra of *epi*-CF₃QD in various solvents. (See SI, Tables S22 and S23, for complete data.)

Table 1. LFER Analysis of Solvent Effects on the Conformational Behavior of Quinidine and Its Derivatives

polarity scale	interacting mechanism	correlation coefficient (R^2)			
		<i>epi</i> -CF ₃ QD <i>syn</i> – <i>anti</i> equilibrium		QD open–closed equilibrium	
		$\Delta G_{\text{syn,exp}}$ (39 solv)	$\Delta G_{\text{syn,cal}}$ (18 solv)	$\Delta G_{\text{open,exp}}$ (18 solv)	$\Delta G_{\text{open,cal}}$ (18 solv)
$(\epsilon - 1)/(\epsilon + 2)$, Y	electrostatic interaction (nonspecific, polarization)	0.350	0.975	0.088	0.998
$(n^2 - 1)/(n^2 + 2)$, P	dispersive interaction (nonspecific, polarizability)	0.237		0.017	
π^*	nonspecific van der Waals interactions (primarily a linear combination of Y and P)	0.001		0.466	
α	H-bond-donating ability (specific)	0.304		0.012	
β	H-bond-accepting ability (specific)	0.814		0.120	
E_{T}^{N}	nonspecific van der Waals and specific H-bonding interactions (an approximately linear combination of π^* , α , and β)	0.317		0.029	
XYZ	a linear combination of P , π^* , α , and β	0.868		0.872	
XYZ'	a linear combination of Y , P , α , and β	0.861		0.554	

conformations appeared upfield. The assignment could be verified by adding CHCl₃ or DMSO into a particular solvent, which led to increase or decrease of the *syn* population, respectively. When deuterated solvents were used, the population distribution could also be measured on the basis of the H9 signals of the *syn* and *anti* conformations in the ¹H NMR, whose relative chemical shifts did not vary with solvent. Using these methods, the *syn*–*anti* conformational distribution of *epi*-CF₃QD in 47 solvents was determined via ¹⁹F NMR peak integrations.^{17a} The open–closed conformational equilibria of QD and *epi*-QD in various solvents were derived based on ³J_{H8H9} coupling constants, which were measured in the corresponding solvents with a concentration of 15 mM at 298 K.

3. RESULT AND DISCUSSION

3.1. Investigation of the Conformations of Quinidine Derivatives via Quantum Chemical Calculations. Figure 1E illustrates the most stable conformers of *epi*-CF₃QD in local minima on the PES. (See SI for all 21 conformers.) The relative energies of fully optimized conformers differ from those indicated on the PES due to different computational methods.

At the B3LYP/6-311+G(d,p) level of theory, seven conformers were identified on the PES of *epi*-QD (Figure 1C). Taking the τ_3 rotation into consideration, the number of conformers increased to 13, and the most stable species of conformers 1–7 are shown in Figure 1F. (See SI for all 13 conformers.) Because of the structural resemblance of QD to cinchonidine (CD), the conformers of QD could be identified with the help of the PES of CD (Figure 1D).^{9d} By including the τ_3 rotation into the conformer exploration, 19 conformers were found (open-11 was not found), and the minimum-energy species of conformers 1–10 are shown in Figure 1G.

As depicted in Figure 1B–D, *epi*-CF₃QD, *epi*-QD, and QD were found to share several similar patterns on their PESs. First, seven major conformers, closed-1, closed-2, open-3, open-4 (open-9 for *epi*-CF₃QD), open-5, open-6, and closed-7, were distributed at relatively similar locations on the PESs of these three molecules, implying their analogous conformational behavior (Figure 1B–D). Second, high barriers to τ_2 rotation have been observed in all three cases, which lead to the kinetic categorization of conformers into two groups, namely, the *syn* and the *anti* conformations. This was particularly important for the conformational study of *epi*-CF₃QD, as it led to two NMR distinguishable signals responsible for the *syn* and the *anti* conformers at room temperature, respectively. The direct measurement of the *syn*–*anti* conformational equilibrium could

thus be achieved through NMR peak integration.¹⁷ Third, barriers to the τ_1 rotations were generally found in the range of a few kcal/mol. With such low rotational barriers, signals of all *syn* (or *anti*) conformers of *epi*-CF₃QD can coalesce into a single peak in the ¹⁹F NMR spectrum, therefore significantly streamlining signal assignment and conformational analysis.

Apart from these similarities, noticeable differences in conformational distributions were also observed. On the PES of QD, only two minima, open-3 and open-4, were found in the zone of $\tau_1 \approx 180$ – 260° (Figure 1D). In comparison, the same region in the PES of *epi*-CF₃QD proved more intricate. Three additional conformers were identified as open-4, open-8, and open-10, corresponding to eclipsed geometry along the C8–C9 bond. Presumably, the energetic cost for forming these seemingly unfavorable conformers is largely reduced by the formation of intramolecular H-bonding and the avoidance of steric interactions between the CF₃ group and the quinoline ring. Compared with the scattered conformational distribution in the region of $\tau_1 \approx 90$ – 120° on the PES of QD, no conformers were identified in the same region for *epi*-CF₃QD. This is presumably due to steric interactions between the CF₃ group and the H18 atom. *epi*-QD was found to be conformationally less diverse than QD and *epi*-CF₃QD (Figure 1C). This can be ascribed to (a) significant stabilization of open-3 and open-4 via intramolecular H-bonding (compared with QD) and (b) less steric congestion around the C8–C9 bond in open-3 and open-4 (compared with *epi*-CF₃QD). Noticeably, while the conformational distribution of *epi*-QD is restricted due to high thermodynamic stabilities of open-3 and open-4 conformers compared with others, PES of *epi*-QD was found to be kinetically shallow, which allows a faster conformational exchange than that of *epi*-CF₃QD.

3.2. Conformational Behavior of *epi*-CF₃QD. **3.2.1. Conformational Study of *epi*-CF₃QD via ¹⁹F NMR.** By introducing the CF₃ group into quinidine, the conformational equilibrium around τ_2 , namely the *syn*–*anti* equilibrium could be investigated in various solvents. According to NOESY spectroscopy, the major species of *epi*-CF₃QD in CDCl₃ were open-3-like (*syn*) conformations, while the minor species adopted open-4-like (*anti*) geometry (Figure 2A).¹⁷ This result is similar to the above-mentioned calculations in the gas phase. The relative populations of these two species were determined to be 83:17 by ¹⁹F NMR integrations, respectively. In DMSO, the

closed-1 and the closed-2 conformations were adopted with a 50:50 ratio (Figure 2B).

Representative results have been shown in Figures 2C,D, and Table 1. In general, high *syn:anti* ratios were seen in solvents possessing low dielectric constants (ϵ), such as pentane ($\epsilon = 1.84$), benzene ($\epsilon = 2.27$), and CHCl_3 ($\epsilon = 4.89$). In contrast, significant stabilization of *anti* conformation was found in solvents with relatively high ϵ , such as acetone ($\epsilon = 21.0$), acetonitrile ($\epsilon = 36.6$), and DMSO ($\epsilon = 47.2$). This trend is consistent with both our theoretical calculations (see Table S22) and previous observations^{3,5,7a} which showed an Onsager-type inverse correlation between the population of open-3-like conformations and ϵ of solvents.

Apart from the agreement of experimental results with calculations, noticeable differences were also observed. Nitrobenzene and nitromethane are “highly polar” solvents based on their dielectric constants ($\epsilon = 35.6$ and $\epsilon = 37.7$, respectively). However, the population of *syn* conformations ($\text{Pop}_{\text{syn,exp}}$) of *epi*- CF_3QD in these two solvents was found to be fairly high (78% and 82%, respectively), which is essentially the same as the $\text{Pop}_{\text{syn,exp}}$ in “non-polar” solvent toluene ($\epsilon = 2.28$, $\text{Pop}_{\text{syn,exp}} = 82\%$, Figure 2C, spectrum 3; Figure 2D, spectra 3 and 4). Despite the fact that water is among the most polar solvent on the dielectric constant polarity scale ($\epsilon = 80.8$), a relatively high $\text{Pop}_{\text{syn,exp}}$ (71%) was observed. Moreover, according to dielectric constants, the conformational behavior of *epi*- CF_3QD in THF ($\epsilon = 7.52$) and pyridine ($\epsilon = 10.4$) was expected to be similar to that in CH_2Cl_2 ($\epsilon = 8.93$). Instead, dramatically different conformational distributions were found, as $\text{Pop}_{\text{syn,exp}} = 65\%$ in THF, $\text{Pop}_{\text{syn,exp}} = 83\%$ in CH_2Cl_2 , and $\text{Pop}_{\text{syn,exp}} = 53\%$ in pyridine. These exceptional results clearly indicate certain deficiencies of dielectric polarity in describing solvent–solute interactions involving *epi*- CF_3QD . In other words, specific interactions, such as H-bonding, may influence the conformational behavior of cinchona alkaloids. It is worth noting that the possible effects of specific interactions were also noticed by Bürgi and Baiker;⁵ however, a clear mechanistic rationale was not achieved due to the paucity of related data.

3.2.2. Elucidation of Solvent Effects Based on Linear Free Energy Relationship (LFER). LFER has been successfully utilized in elucidating complicated chemical processes and interactions, such as asymmetric catalysis²⁵ and solvent–solute interactions.^{26b,27} In principle, the establishment of a good linear relationship with a solvent polarity scale indicates the predominance of the corresponding solvent–solute interaction in a chemical process or equilibrium. A systematic exploration of solvent effects on the *syn*–*anti* equilibrium of *epi*- CF_3QD was performed by means of LFER.²⁶ To examine the accuracy of the previously proposed Onsager function²⁸ in predicting cinchona alkaloid conformational distribution,⁵ we attempted to establish a linear correlation of $\Delta G_{\text{syn,exp}}$ with $(\epsilon - 1)/(\epsilon + 2)$ (denoted by Y).²⁹ However, only a weak correlation ($R^2 = 0.351$) was obtained with 39 data points (Figure 3C, Table 2; see SI for details), therefore excluding electrostatic interaction as the dominant solvent effect influencing the *syn*–*anti* equilibrium. Plotting the previously reported $\Delta G_{\text{open-3}}$ of CD^{5,30} against $(\epsilon - 1)/(\epsilon + 2)$ led to a similarly weak correlation ($R^2 = 0.361$). Both of these results are in agreement with the notion that specific interactions can significantly influence the conformational behavior of cinchona alkaloids and their derivatives (see SI for details).

To describe the complicated solvent effects, a multiparameter approach, incorporating both specific and nonspecific aspects of

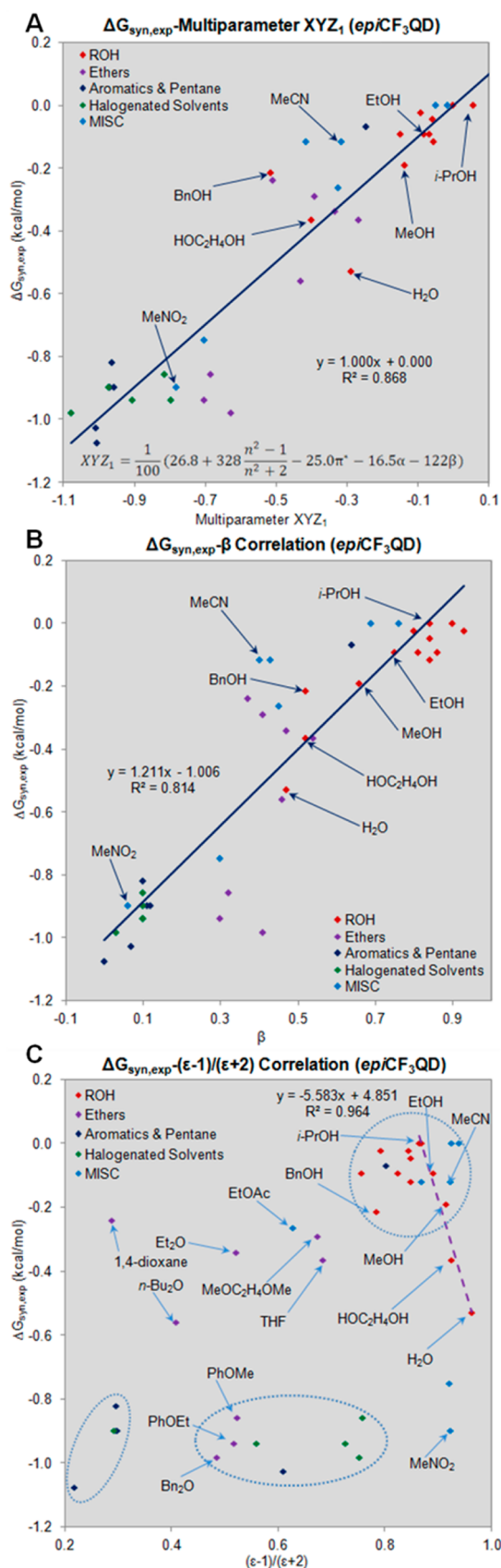


Figure 3. (A) Correlation of $\Delta G_{\text{syn,exp}}$ of *epi*- CF_3QD with multiparameter polarity scale XYZ_1 . (B) Correlation of $\Delta G_{\text{syn,exp}}$ of *epi*- CF_3QD with H-bond-accepting ability (β) of various solvents. (C) Plot of $\Delta G_{\text{syn,exp}}$ of *epi*- CF_3QD versus $(\epsilon - 1)/(\epsilon + 2)$ of various solvents (dielectric interaction).

Table 2. Calculated Properties of Different Conformers of *epi*-QD in the Gas Phase^a

conformer	ΔG (kcal/mol) ^b	Pop (%) ^c	φ_{H8H9} ^d	J_{H8H9} (Hz) ^e	$J_{\text{H8H9}} \times \text{Pop}$ (Hz) ^f
closed-1a	5.6	0.0	299.4	3.41	0.0
closed-1b	3.8	0.1	299.0	3.36	0.0
closed-2b	5.1	0.0	293.9	2.80	0.0
closed-7c	4.6	0.0	290.1	2.41	0.0
open-3a	0.0	67.8	185.3	8.81	6.0
open-3b	4.7	0.0	169.5	8.40	0.0
open-4a	0.4	31.9	184.8	8.84	2.8
open-4b	4.9	0.0	165.6	8.02	0.0
open-4c	8.6	0.0	165.6	8.02	0.0
open-6a	4.9	0.0	60.1	3.47	0.0
open-6b	3.5	0.2	60.3	3.45	0.0
open-5a	7.5	0.0	62.8	3.71	0.0
open-5b	5.6	0.0	60.0	3.48	0.0

^aCalculated at the M06-2X/6-311+G(d,p)//B3LYP/6-311+G(d,p) level. ^bGibbs free energies relative to open-3a. ^cPopulation. ^dDihedral angle of H8–C9–C8–H9. ^ePredicted J_{H8H9} based on modified Karplus equation. ^fThe coupling constant contribution of each conformer to the overall J_{H8H9} .

solvation by means of linear combination, is necessary.^{26b,27b,31} In particular, H-bonding interactions are expected to be significant due to the presence of the quinoline/quinuclidine and the hydroxyl functionalities. Based on this analysis, the multiparameter expression should be composed of at least four independent parameters, namely, (a) the polarization term $(\epsilon - 1)/(\epsilon + 2)$ (reflects electrostatic interaction, Y),^{26b} (b) the polarizability term $(n^2 - 1)/(n^2 + 2)$ (reflects London's dispersive force, denoted by P),^{26b} and (c and d) the H-bond-donating and -accepting ability α and β .³²

Since overall nonspecific solvent–solute interactions can be approximated by the empirical polarity scale π^* (primarily a blend of Y and P) with a polarizability correction term $p \cdot (n^2 - 1)/(n^2 + 2)$,³³ a multiparameter polarity scale was devised as³⁴

$$XYZ = XYZ_0 + a \cdot \alpha + b \cdot \beta + s \cdot \pi^* + p \cdot P$$

where XYZ_0 , a , b , s , and p are solvent-independent regression coefficients and indicative of the sensitivity of the conformational equilibrium toward the corresponding solvent property.

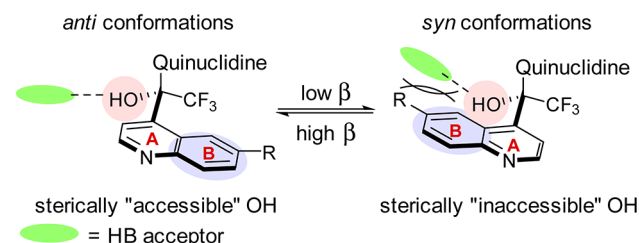
This equation resembles the well-known Kamlet–Taft expression.³² In comparison, the quality of XYZ , XYZ' ($XYZ' = XYZ_0' + a \cdot \alpha + b \cdot \beta + y \cdot Y + p \cdot P$) scales and the empirical polarity scale E_T^{N35} were also investigated. On the XYZ scale, the nonspecific polarity term $s \cdot \pi^* + p \cdot P$ accounts for solvation induced by solvent dipoles, quadrupoles, higher multipoles and dispersive forces. On the XYZ' scale, because the nonspecific polarity term $y \cdot Y + p \cdot P$ can only describe dipolar and dispersive interactions, the XYZ' scale differs from the XYZ scale mainly by the absence of quadrupolar and higher multipolar interactions.^{33b}

Table 1 and Figure 3A show a good linearity between $\Delta G_{\text{syn,exp}}$ and the XYZ_1 polarity scale ($R^2 = 0.868$). A good correlation was also obtained with the XYZ_1' scale, which excludes effects induced by solvent quadrupoles and higher multipoles. In contrast, $\Delta G_{\text{syn,exp}}$ was found to weakly correlate with E_T^N ($R^2 = 0.317$; see SI for details). In spite of the weak dependence of $\Delta G_{\text{syn,exp}}$ with single parameters Y , P , π^* , and α ,

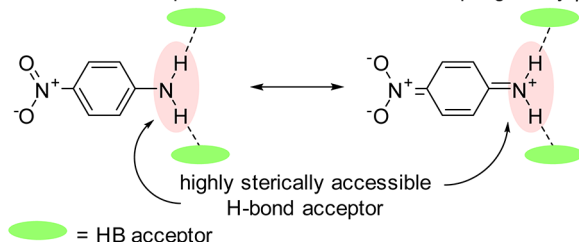
the H-bond-accepting ability of solvents (β) was found to well correlate to $\Delta G_{\text{syn,exp}}$ ($R^2 = 0.814$). The coefficient of the $\Delta G_{\text{syn,exp}} - \beta$ correlation was essentially the same as that of the $\Delta G_{\text{syn,exp}} - XYZ$ correlation, revealing the predominance of the H-bond-accepting ability of solvents in overall solvent effects (Figure 3B).

The positive correlation of $\Delta G_{\text{syn,exp}}$ with β in Figure 3B indicates that the *syn* conformations are stabilized in solvents with low β values. This observation can be explained by the different steric environments around the hydroxyl group in the *syn* and the *anti* conformations (Figure 4A). In the *syn*

A. Plausible role of β in the *syn-anti* conformational equilibrium



B. Solvatochromic probe for solvent H-bond accepting ability β



C. Steric effect of solvents on conformational distribution

Example 1:

β	PhOMe, PhOEt, (PhCH ₂) ₂ O	<i>n</i> -Bu ₂ O	Et ₂ O, 1,4-dioxane, MeOC ₂ H ₄ OMe, THF
$\Delta G_{\text{syn,exp}}$ (kcal/mol)	0.30–0.41	0.46	0.37–0.54
	-0.86 - -0.98	-0.56	-0.24 - -0.37

steric hindrance around the O atom decreases

Example 2:

β	Me-C≡N	Me-C(=O)-Me	Me-C(=O)-O-Me	Me-O-C(=O)-Me
$\Delta G_{\text{syn,exp}}$ (kcal/mol)	0.40	0.43	0.45	0.47
	-0.12	-0.12	-0.27	-0.34

steric hindrance around the HB accepting site increases

Figure 4. (A) Plausible role of H-bonding interaction in the *syn-anti* conformational equilibrium. (B) Determination of H-bond-accepting ability (β) using solvatochromic probe, in which the H-bond acceptor possesses less steric encumbrance than the hydroxyl group in *epi*-CF₃QD. (C) Steric effect of solvents on the conformational distribution. $\Delta G_{\text{syn,exp}}$ varies significantly with relatively unchanged β values, revealing that the steric hindrance around solvents' H-bond-accepting sites can influence the conformational distribution of *epi*-CF₃QD.

conformations, the hydroxyl group is sterically insulated by the quinoline ring and thus less involved in H-bonding interaction. In contrast, the hydroxyl group in the *anti* conformation is an effective H-bond donor due to its higher accessibility. The H-bonding thus tends to stabilize *anti* conformations more than its *syn* counterparts. In general, hydrocarbon-based solvents and

their halogenated derivatives are poor H-bonding acceptors. Neither *syn* nor *anti* conformations are stabilized in these solvents through specific interactions; this results in large energy differences as observed in the gas phase (ca. -1.0 kcal/mol). Some ethers, such as diethyl ether (Et_2O), di-*n*-butyl ether (*n*- Bu_2O), and THF, possess moderate H-bond acceptance, thus leading to moderate $\Delta G_{\text{syn,exp}}$ values by stabilizing *anti* conformations (ca. -0.4 kcal/mol). Such $\Delta G_{\text{syn,exp}}-\beta$ correlation was particularly strong in protic solvents, i.e. H_2O , ethylene glycol, MeOH, EtOH, and *i*-PrOH (Figure 3B).

Apart from these good linear relationships, noticeable deviations of $\Delta G_{\text{syn,exp}}$ from the β -scale were also observed. For example, according to β values, all ethers of interest possess similar H-bond-accepting abilities ($0.30 < \beta < 0.54$); nevertheless, significantly higher $\Delta G_{\text{syn,exp}}$ values were observed in aromatic ethers than in saturated ethers (Figure 4C, example 1). Since the β -scale was derived on the basis of the H-bonding interaction of sterically “non-hindered” *p*-nitroaniline (and other structurally similar probes), the steric effects of H-bond acceptors on β values should be minimal (Figure 4B). In comparison, the hydroxyl group in *epi*- CF_3QD is located in a rather crowded environment. Its H-bonding interaction with ethers is expected to decrease as the steric hindrance around the ethereal oxygen atom increases (aromatic ether $>$ *n*- Bu_2O $>$ other ethers). Similarly, although acetonitrile, acetone, ethyl acetate, and Et_2O have similar β values, their stabilizing effects on the *anti* conformations were found to gradually decrease with the increase in the steric encumbrance around the H-bond-accepting site (Figure 4C, example 2).

It is worth noting that the importance of H-bonding interactions on the conformational equilibrium of *epi*- CF_3QD can also be inferred by the conformational behavior of its *O*-methylated derivatives (*epi*- MeOCF_3QD).^{17b} ^{19}F NMR spectroscopy shows that the *syn* population of *epi*- MeOCF_3QD is almost constant ($>95\%$) in solvents with various β values (see SI for details). Such an observation may be attributed to both the steric congestion around the C9 atom and the absence of the OH-solvent-specific interactions, which govern the conformational behavior of *epi*- CF_3QD .

Regarding the $\Delta G_{\text{syn,exp}}-(\epsilon - 1)/(\epsilon + 2)$ correlation, the most significant data scattering was found in the moderate polarity region ($0.3 < (\epsilon - 1)/(\epsilon + 2) < 0.7$). We ascribed this observation to the incapability of $(\epsilon - 1)/(\epsilon + 2)$ in describing steric effects and H-bond-accepting ability. For example, although the introduction of C- NO_2 and C-Cl dipolar moieties can increase the ϵ of many solvents, these moieties are weak H-bonding acceptors. Such mismatching thus leads to significant deviation in $\Delta G_{\text{syn,exp}}-(\epsilon - 1)/(\epsilon + 2)$ correlation in halogenated and nitro-containing solvents.

In contrast, a close association of $\Delta G_{\text{syn,exp}}$ with dielectric constant polarity was found in solvents possessing high or low ϵ values. Large $\Delta G_{\text{syn,exp}}$ (ca. -1.0 to -0.8 kcal/mol) values were commonly observed in solvents with $(\epsilon - 1)/(\epsilon + 2)$ values $<$ 0.3, whereas $\Delta G_{\text{syn,exp}}$ became rather small (ca. 0.0 to -0.3 kcal/mol) with high $(\epsilon - 1)/(\epsilon + 2)$ values ($>$ 0.7). Although this trend appears in good agreement with the previous conclusion by Bürgi and Baiker, such consistency may just simply be due to the positive interrelation between the β and the ϵ scales. Strong H-bond-accepting ability generally necessitates significant charge separation within solvent molecules (such as DMSO and DMF), which in turn leads to high ϵ values. On the other hand, solvents containing no

dipolar moieties, such as hydrocarbons, usually have both low dielectric constants and weak H-bond-accepting ability.

Good linearity ($R^2 = 0.964$) was established between $\Delta G_{\text{syn,exp}}$ and $(\epsilon - 1)/(\epsilon + 2)$ in the family of simple alcohols (water, ethylene glycol, MeOH, EtOH, *n*-PrOH and *i*-PrOH), as $\Delta G_{\text{syn,exp}}$ decreased with the increase in dielectric constant. Moreover, a strong negative correlation ($R^2 = 0.969$) was also found between β and $(\epsilon - 1)/(\epsilon + 2)$ of simple alcohols. Gas-phase calculations have shown that binding energies of aniline (as a donor) with water, MeOH, EtOH and *n*-PrOH (as acceptors) are essentially the same; namely, their “intrinsic” H-bond-accepting abilities are identical (see SI for details). This implies that the different empirical H-bond-accepting abilities (β) of these alcohols mainly originate from their dielectric constants rather than the strength of the O–H bond. In other words, with increased dielectric constant, an alcoholic solvent tends to solvate itself more strongly via dipolar interaction, therefore leading to the decrease in their H-bond acceptance to *epi*- CF_3QD . Due to practically the same “intrinsic” H-bond-accepting abilities of simple alcohols, solvation energies of the *syn* and the *anti* conformers in these solvents are anticipated to primarily correlate with $(\epsilon - 1)/(\epsilon + 2)$. This result shows that the Onsager function is applicable only in cases where the influence of other interactions is similar or negligible.

3.2.3. Comparison of Theoretical Calculations with Experimental Data. Based on the DFT calculations mentioned in section 2.1, $\Delta G_{\text{syn,cal}}$ of *epi*- CF_3QD obtained in 18 solvents was plotted against the corresponding $\Delta G_{\text{syn,exp}}$, which yielded a correlation with a R^2 value of 0.381 (Figure 5A, red line). On the other hand, although the PCM model exploits a formalization different from that of the simple Onsager model to calculate solvent effects,²² $\Delta G_{\text{syn,cal}}$ was found to be strongly correlated to the Onsager-like function $(\epsilon - 1)/(\epsilon + 2)$ ($R^2 = 0.967$) only with small deviation. Because of this, the weak correlation between $\Delta G_{\text{syn,exp}}$ and $\Delta G_{\text{syn,cal}}$ can be ascribed to the inconsistency of $(\epsilon - 1)/(\epsilon + 2)$ with β , as confirmed by the resemblance of the $\beta-(\epsilon - 1)/(\epsilon + 2)$ plot to the $\Delta G_{\text{syn,exp}}-\Delta G_{\text{syn,cal}}$ plot (through a clockwise rotation of 180° , Figure 5A has pattern very similar to that of Figure 5C). As depicted, $\Delta G_{\text{syn,exp}}$ and $\Delta G_{\text{syn,cal}}$ significantly diverged when β and $(\epsilon - 1)/(\epsilon + 2)$ values are “mismatched” (Figure 5A,C, red spots without circles).

Noticeably, even though $\Delta G_{\text{syn,exp}}$ and $(\epsilon - 1)/(\epsilon + 2)$ were found to be positively correlated in alcohols (see SI for details), theory predicted an opposite solvent-dependence trend (Figure 5B). In our PCM-based calculations, *epi*- CF_3QD predominantly interacts with the solvent through an Onsager-type behavior. This may differ from the actual solvation, in which the H-bonded *epi*- CF_3QD -alcohol complexes (or alcohol solvent shell) interact with solvent molecules through an interaction similar to Onsager-type description, which can probably explain the opposite predication of solvent effects.

3.3. Conformational Behavior of *epi*-QD in Various Solvents. As mentioned in section 3.1, DFT calculations have provided the $\Delta G_{\text{open,cal}}$ of 13 *epi*-QD conformers in the gas phase. Two major conformers were identified in the gas phase as open-3a and open-4a, with relative energies of 0.0 and 0.4 kcal/mol, respectively (Table 2). Other than these two species, all other conformers are energetically unfavorable ($\Delta G >$ 3.5 kcal/mol). Similar to *epi*- CF_3QD , the intramolecular quinuclidine-N \cdots H–O H-bonding has been found in open-3a and open-4a as indicated by the short N–H contacts. According to second-order perturbation theory analysis,²⁴ the donor (lone

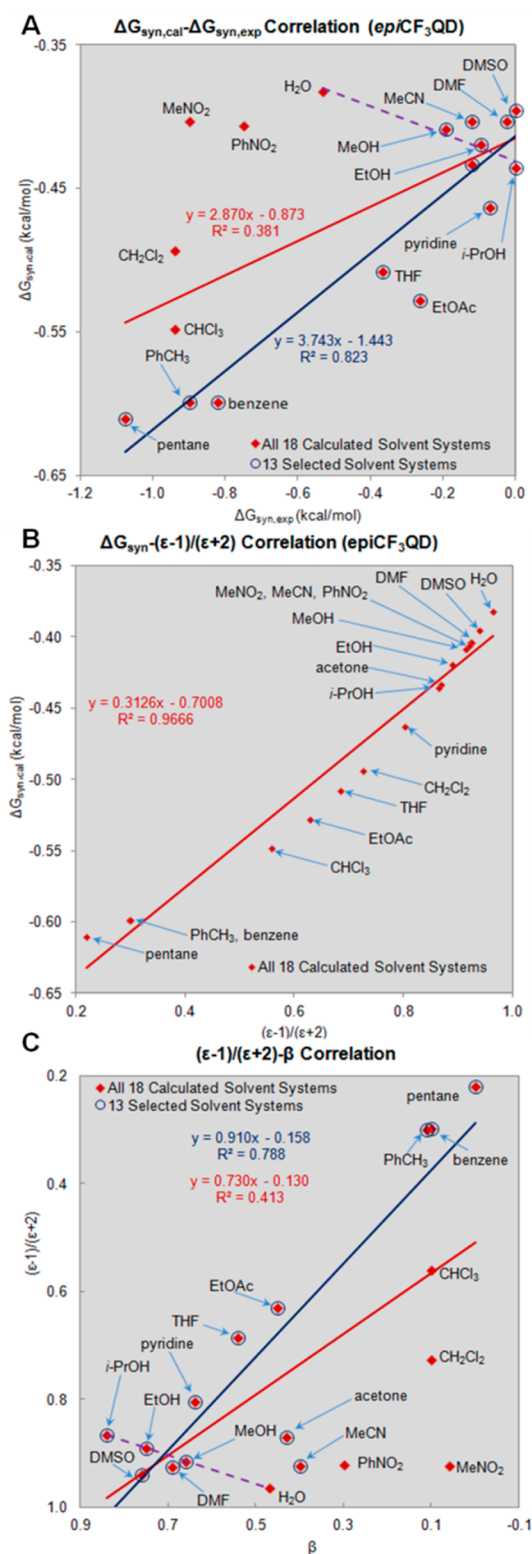


Figure 5. (A) Correlation of $\Delta G_{\text{syn,exp}}$ of *epi*-CF₃QD with $\Delta G_{\text{syn,cal}}$; five uncircled calculated $\Delta G_{\text{syn,cal}}$ values significantly diverge from the experimental data (B) Correlation of $\Delta G_{\text{syn,cal}}$ of *epi*-CF₃QD with $(\epsilon - 1)/(\epsilon + 2)$ of various solvents (dipolar interaction). (C) Correlation of $(\epsilon - 1)/(\epsilon + 2)$ with β , which shows a scattered pattern similar to that shown in panel A.

pair on N)—acceptor ($\sigma_{\text{O-H}}^*$) interaction energies are around 0.5 kcal/mol or less, which are significantly weaker than the internal H-bonding in open-3a of *epi*-CF₃QD (5.7 kcal/mol).

Because the N...H distances and N...H—O bond angles in *epi*-QD conformers are close to the corresponding values in open-3a of *epi*-CF₃QD, the significantly smaller interaction energy can be attributed to the weaker acidity of the OH group in *epi*-QD.

As shown in Table 3, the population summation of open-3 and open-4 was calculated to be >99.6% in solvents under

Table 3. PCM-Based Calculated Conformational Distribution of *epi*-QD in Various Solvents^a

solvent	Pop _{open-3} /Pop _{open-4} (%/%) ^{a,b}	$\Delta G_{\text{open-3}}$ (kcal/mol) ^a	$J_{\text{H8H9,cal}}$ (Hz) ^c	$J_{\text{H8H9,exp}}$ (Hz) ^d
benzene	61.9/37.8	-0.29	8.8	9.8
toluene				9.8
CHCl ₃	57.5/42.3	-0.18	8.8	9.8
CH ₂ Cl ₂				9.9
THF	55.4/44.3	-0.13	8.8	9.7
<i>i</i> -PrOH				9.8
acetone				9.8
EtOH				9.4
MeOH	51.4/48.3	-0.03	8.8	9.3
PhNO ₂				9.8
MeCN	51.3/48.4	-0.03	8.8	9.5
MeNO ₂				9.9
DMF				9.8
DMSO	51.0/48.7	-0.02	8.8	9.0
H ₂ O	50.5/49.1	-0.01	8.8	9.3

^aCalculated at the PCM-M06-2X/6-311+G(d,p)//B3LYP/6-311+G(d,p) level of theory. ^bAccording to the calculation, open-3 and open-4 were found to be the major conformers, and the overall population of other conformers ranges from 0.2% to 0.4% in various solvents. ^cPredicted J_{H8H9} based on modified Karplus equation and calculated dihedral angle of H8—C9—C8—H9 (φ_{H8H9}). ^dMeasured by ¹H NMR (500 MHz) in deuterated solvents.

investigation, and the $\Delta G_{\text{open-3}}$ was obtained on the basis of the corresponding Pop_{open-3}/Pop_{open-4} values. Plotting the $\Delta G_{\text{open-3}}$ against $(\epsilon - 1)/(\epsilon + 2)$ led to a perfect linearity ($R^2 = 1.000$), which resembles the Onsager function.²⁸ To quantify the population distribution of *epi*-QD in different solvents, we adopted a method described by Baiker et al.,⁵ which assumed the observed J_{H8H9} to be a weighted averaged coupling constant of all conformers, namely $\sum(\text{Pop}_{(i)} \times J_{\text{H8H9}(i)})$. Moreover, with calculated H8—C9—C8—H9 dihedral angles ($\varphi_{\text{H8H9}(i)}$) in hand, the corresponding vicinal coupling constants ($J_{\text{H8H9}(i)}$) of different conformers (*i*) were obtained via a modified Karplus equation,³⁶ in which both substituent and stereochemistry effects are taken into consideration.

Given the facts that the observed J_{H8H9} was almost constant in all solvents and open-3 and open-4 had essentially the same J_{H8H9} , these two gas-phase-abundant conformers should be dominant in all solvents. This result is in good agreement with our calculated coupling constant, in which J_{H8H9} was shown to be solvent-independent (Table 3). Hence, it can be concluded that conformers with $\Delta G > 3.5$ kcal/mol in the gas phase were unlikely to be significantly populated in solution. The NOESY of *epi*-QD in CD₂Cl₂ and DMSO-*d*₆ also identified both open-3 and open-4 as major conformers with very similar correlation patterns, revealing that the Pop_{open-3}/Pop_{open-4} ratio did not change significantly in different solvents (see SI for details). According to the gas-phase calculations at the B3LYP/6-311+G(d,p) level, open-3 and open-4 possessed very similar dipole moments (5.20 and 5.42 D, respectively). Thus, the

dipolar interaction on the conformational equilibrium should be insignificant.

3.4. Conformational Behavior of QD in Various Solvents. QD is conformationally more flexible than *epi*-QD. This is not only reflected by its higher number of conformers (19 minimum energy conformers were found for QD), but also by its shallower PES in the gas phase (Table 4). Compared with

Table 4. Calculated Properties of Different Conformers of QD in the Gas Phase^a

conformer	ΔG_{cal} (kcal/mol) ^b	Pop (%) ^c	φ_{H8H9} ^d	J_{H8H9} (Hz) ^e	$J_{\text{H8H9}} \times \text{Pop}$ (Hz) ^f
closed-1a	3.1	0.4	175.4	9.15	0.0
closed-1b	1.2	9.2	173.3	9.13	0.8
closed-2a	3.3	0.3	175.6	9.15	0.0
closed-2b	1.8	3.6	176.0	9.15	0.3
closed-7a	4.1	0.1	179.8	9.11	0.0
closed-7b	2.4	1.3	178.9	9.13	0.1
closed-7c	2.0	2.6	179.6	9.11	0.2
open-3b	0.0	74.4	78.3	0.95	0.7
open-3c	2.3	1.7	82.5	0.92	0.0
open-4a	4.0	0.1	60.2	1.89	0.0
open-4b	3.1	0.4	80.7	0.92	0.0
open-9b	3.3	0.3	80.4	0.92	0.0
open-9c	3.2	0.3	81.3	0.92	0.0
open-5b	4.3	0.1	281.4	1.38	0.0
open-6a	4.7	0.0	293.8	2.27	0.0
open-6b	2.9	0.5	287.2	1.73	0.0
open-6c	3.5	0.2	315.3	4.58	0.0
open-8c	9.0	0.0	316.6	4.72	0.0
open-10c	1.4	6.5	317.1	4.78	0.3

^aCalculated at the M06-2X/6-311+G(d,p)//B3LYP/6-311+G(d,p) level of theory. ^bGibbs free energies relative to open-3b. ^cRelative population. ^dDihedral angle of H8–C9–C8–H9. ^ePredicted J_{H8H9} obtained via modified Karplus equation. ^fThe coupling constant contribution of each conformer to the overall J_{H8H9} .

epi-QD, which only had two conformers possessing $\Delta G < 3.0$ kcal/mol, eight conformers were found for QD within that energy range. Similar to cinchonidine,^{5,9d} open-3b, closed-1b, closed-2b, closed-7c, and open-10c were identified to be important conformers with population higher than 2%. Differing from *epi*-CF₃QD and *epi*-QD, the stereochemistry of QD does not allow the formation of internal H-bonding in its open-3 conformation (Figure 1G). Instead, sterically unfavorable open-10c was found to be stabilized by internal H-bonding, which provides a stabilization of 3.0 kcal/mol as indicated by the second-order perturbation theory NBO analysis.²⁴

$\Delta G_{\text{open,cal}}$ in various solvents was calculated on the basis of the overall population of open conformations, i.e., open-3–8 and open-8–10. The $\Delta G_{\text{open,cal}}$ of QD was found to well correlate with $(\epsilon - 1)/(\epsilon + 2)$ of 13 solvents with $R^2 = 0.998$ (Figure 6B). The population of open-3b significantly decreases with the increase in ϵ of solvents, while the population of closed conformers generally increases in solvents with high dielectric constant. This result could be ascribed to the relatively lower dipole moment of open-3b ($\mu = 2.65$ D in the gas phase) compared with other conformers ($\mu > 3.12$ D in the gas phase).

To quantify the population distribution of QD in solvents via J_{H8H9} analysis, we adopted the two-equation, two-variable linear

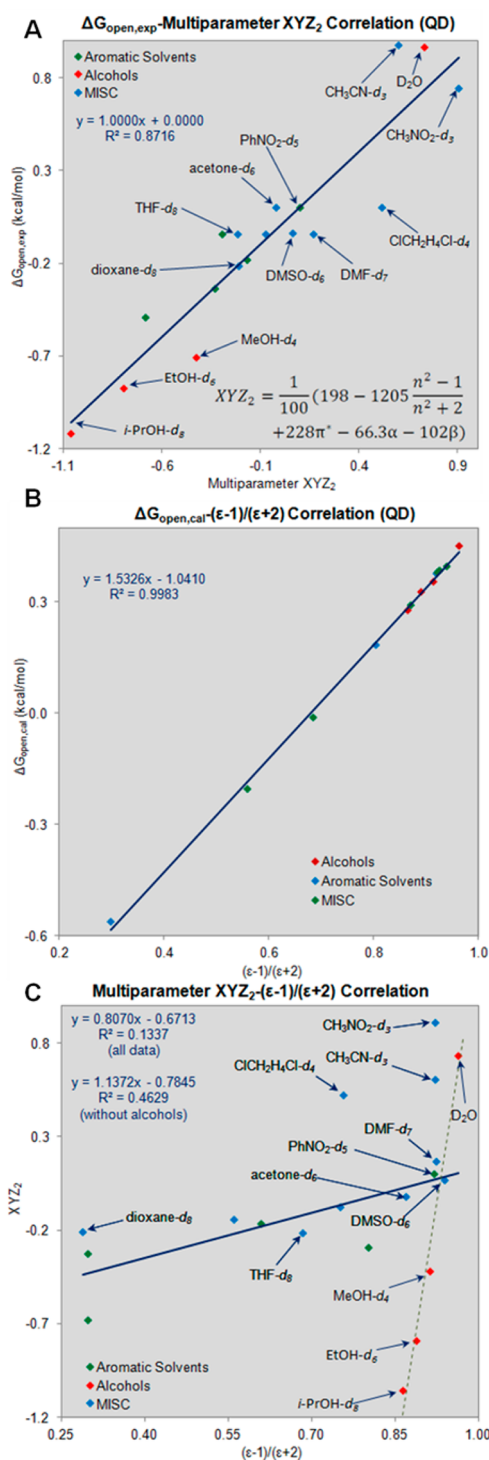


Figure 6. (A) Correlation of $\Delta G_{\text{open,exp}}$ with multiparameter XYZ₂. (B) Correlation of $\Delta G_{\text{open,cal}}$ of QD with $(\epsilon - 1)/(\epsilon + 2)$ of various solvents (dielectric interaction). (C) Correlation of multiparameter XYZ₂ with $(\epsilon - 1)/(\epsilon + 2)$.

system described by Baiker et al.⁵ As the closed conformations had essentially the same coupling constant, the linear system involved two equations and at least three variables, $\text{Pop}_{\text{open-3}}$, $\text{Pop}_{\text{closed}}$, and $\text{Pop}_{\text{open-10}}$ (eqs 5 and 6).

$$J_{\text{H8H9}}^{\text{obs}} = J_{\text{H8H9}}^{\text{open-3}} \times \text{Pop}_{\text{open-3}} + J_{\text{H8H9}}^{\text{closed}} \times \text{Pop}_{\text{closed}} + J_{\text{H8H9}}^{\text{open-10}} \times \text{Pop}_{\text{open-10}} \quad (5)$$

$$\text{Pop}_{\text{open-3}} + \text{Pop}_{\text{closed}} + \text{Pop}_{\text{open-10}} = 1 \quad (6)$$

where $J_{\text{H8H9}}^{\text{obs}}$ is the observed J_{H8H9} ; $J_{\text{H8H9}}^{\text{open-3}}$, $J_{\text{H8H9}}^{\text{closed}}$, and $J_{\text{H8H9}}^{\text{open-10}}$ are J_{H8H9} of open-3, closed, and open-10 conformations, respectively. $\text{Pop}_{\text{open-3}}$, $\text{Pop}_{\text{closed}}$, and $\text{Pop}_{\text{open-10}}$ are populations of open-3, closed, and open-10 conformers, respectively.

According to NOESY spectrum, open-10c was not a major conformer in solution, which was consistent with both the present and the previous PCM calculations.^{9d} Moreover, it was anticipated that the population of open-10c could further decrease because of diminishing internal H-bonding in H-bond-accepting solvents. Therefore, with moderate J_{H8H9} values and low population, open-10c was estimated to have negligible influence on the observed vicinal couplings (<0.5 Hz). The exclusion of the contribution from open-10c thus led to systematic errors in conformational distribution quantification, which did not significantly affect the trend of solvent dependence. On this basis, a two-equation, two-variable linear system similar to the previous expression⁵ was formulated (eq 1 and eq 2), which allowed the determination of $(\text{Pop}_{\text{open}}/\text{Pop}_{\text{closed}})_{\text{exp}}$ via J_{H8H9} analysis (Table 5). $\Delta G_{\text{open,exp}}$ in 18 solvents was thus obtained.

Table 5. Conformational Distribution of QD and $\Delta G_{\text{open,exp}}$ in Various Solvents

solvent	$J_{\text{H8H9,exp}}$ (Hz) ^{a,b}	$\text{Pop}_{\text{open,exp}}$ (%) ^c	$\Delta G_{\text{open,exp}}$ (kcal/mol) ^d	$\Delta G_{\text{open,cal}}$ (kcal/mol) ^e
dioxane	4.3	59	-0.21	
benzene	3.9	64	-0.34	-0.56
<i>p</i> -xylene	3.4	70	-0.49	
PhCl	4.4	58	-0.18	
THF	4.9	52	-0.04	-0.0
<i>o</i> -C ₆ H ₄ Cl ₂	4.9	52	-0.04	
ClC ₂ H ₄ Cl	5.4	46	0.10	
pyridine	4.9	52	-0.04	0.18
<i>i</i> -PrOH	2.0	87	-1.12	0.28
acetone	5.4	46	0.10	0.29
EtOD	2.5	81	-0.88	0.36
MeOD	2.8	77	-0.71	0.35
PhNO ₂	5.4	46	0.10	0.38
MeCN	7.8	16	0.97	0.38
MeNO ₂	7.3	22	0.74	0.38
DMF	4.9	52	-0.04	0.38
DMSO	4.9	52	-0.04	0.40
H ₂ O	7.3	22	0.74	0.45

^aObserved J_{H8H9} , measured by ¹H NMR (500 MHz) in deuterated solvents as indicated. ^bSignificant line broadening of the H8 signal (d) was observed in many cases, which leads to difficulty in the determination of $J_{\text{H8H9,exp}}$. Under such circumstance, $J_{\text{H8H9,exp}}$ was achieved by measuring the coupling constant of the doublet of the H9 signal (td). ^cPopulation of open conformations based on $J_{\text{H8H9,exp}}$ and modified Karplus equation. ^dBased on the Boltzmann equation and $\text{Pop}_{\text{open,exp}}$ data. ^e $\Delta G_{\text{open,cal}} = -RT \ln(\sum \text{Pop}_{\text{open}}/\sum \text{Pop}_{\text{closed}})$.

Even though $\Delta G_{\text{open,exp}}$ was almost independent of $(\epsilon - 1)/(\epsilon + 2)$ ($R^2 = 0.088$, Table 1), a good correlation was found within the family of alcoholic solvents. As discussed in section 3.2.3, such an observation can be presumably rationalized by the similar contribution from the specific solvent–solute interactions to the overall solvation energy.

On the other hand, a good linear relationship of $\Delta G_{\text{open,exp}}$ was established with multiparameter XYZ_2 , which was a linear combination of α , β , π^* , and a polarizability correction term $p \cdot P$

($R^2 = 0.872$) (Figure 6A and Table 2). In contrast, the multiparameter XYZ_2' , namely $\text{XYZ}_0' + y \cdot Y + p \cdot P + a \cdot \alpha + b \cdot \beta$, correlated with $\Delta G_{\text{open,exp}}$ to give a relatively lower $R^2 = 0.554$. The poorer correlation is presumably owing to the absence of significant quadrupole and higher multipole terms. To assess the reliability of PCM-based calculations, XYZ_2 was plotted against $(\epsilon - 1)/(\epsilon + 2)$ to yield a very weak correlation (Figure 6C). Evidently, the present PCM calculations, practically resembling the Onsager function, is not sufficiently accurate to describe the overall solvation of QD, which involves interacting mechanisms other than dielectric interaction.

Figure 7A demonstrates the contribution from individual polarity parameter to the multiparameter XYZ_2 . According to

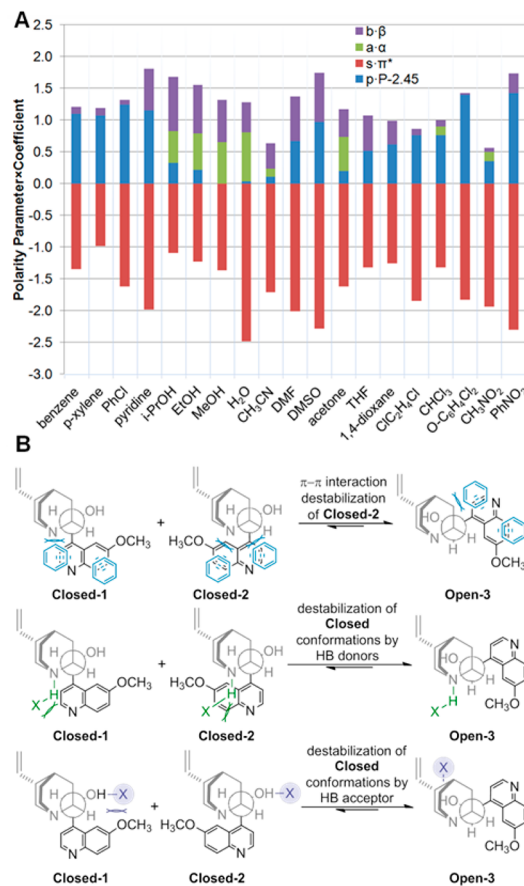


Figure 7. (A) Contribution from individual solvent properties to the multiparameter XYZ_2 . α and β represent H-bond-donating ability, respectively. π^* describes nonspecific van der Waals interactions. P represents dispersive interactions. (B) Rationalization of stabilization/destabilization from solvent–solute interactions.

the large values of $s \cdot \pi^*$ terms, aromatic solvents were as “polar” as other solvents, such as CH₃CN and CH₃NO₂, thus leading to the expectation of large ΔG_{open} . However, the high π^* polarity of aromatic solvents was largely compensated for polarizability correction term $p \cdot P$ (Figure 7A, notice the significant blue bars ($p \cdot P$) of aromatic solvents compared with the small $p \cdot P$ values of CH₃CN and CH₃NO₂). This implies that the open conformations (mainly open-3) were stabilized by dispersive interaction (Figure 7B).³⁷ Such effects were particularly notable for the conformational equilibrium in CH₃NO₂ and PhNO₂, as Pop_{open} was found doubled in the latter (Table 5). The overall H-bonding interaction was

approximately the same in H₂O and in alcohols (notice purple bars and green bars of alcohols in Figure 7A). Therefore, the significant destabilization of open conformations in H₂O, compared with other alcohols, is primarily due to nonspecific interactions (notice red bars of alcohols in Figure 7A).

Based on the multiparameter dissection, it is also obvious that the exceptionally high Pop_{open} in alcohols is due to both H-bond-accepting and -donating capacity of the solvents, which cancels out the effects due to other nonspecific van der Waals interactions (*s*- π + *p*-*P*). Similar to the observation with *epi*-CF₃QD, the H-bond-accepting ability of solvents was also found to stabilize the *anti* conformations of QD (open-3, Figure 3B). The relatively weak impact of β on the conformational equilibrium of QD is in part due to the lower acidity of the OH group and the absence of intramolecular H-bonding in major conformers. The stabilization of open conformations by H-bonding donation from solvents can be rationalized by the higher accessibility of the quinuclidine nitrogen in the respective conformations (Figure 3B).

4. THE INFLUENCE OF SOLVENT-INDUCED CONFORMATIONAL BEHAVIOR OF QD IN S_N2 REACTION, A CASE STUDY

As mentioned above, the links between the conformation and the catalytic activity/reactivity of cinchona alkaloids have been well documented in the literature.^{1f,3-9} Herein, a model S_N2 reaction, as an additional example to other well-known studies, is presented to address the influence of solvent-induced conformational change of QD on its reactivity toward α -bromoacetate (Figure 8A). Similar S_N2 reactions have been shown to be critical for many catalytic and synthetic processes, such as Gaunt's enantioselective catalytic cyclopropanation

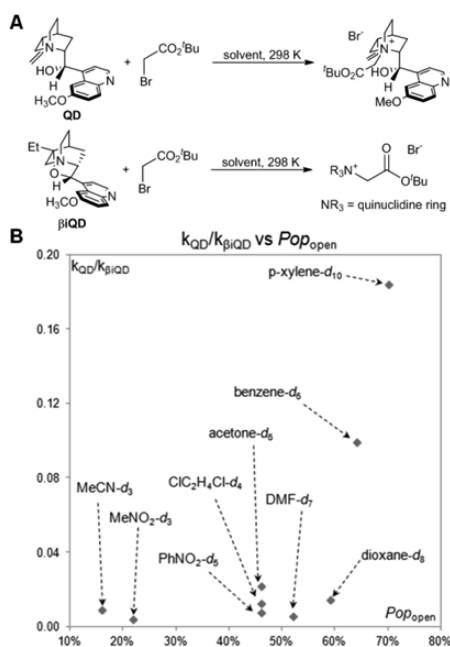


Figure 8. (A) Reactions between quinidine/ β -isoquinidine and α -bromoacetate. (B) The influence of population of open conformations of quinidine on reaction rates. k_{QD} and $k_{\beta iQD}$ are the rate constant of the reaction of QD and β -iQD with α -bromoacetate, respectively. Pop_{open} is the population of open conformations in the corresponding solvent. See Table 5.

reaction³⁸ and the synthesis of various cinchona alkaloid-based phase-transfer catalysts.^{1f}

As the rate of S_N2 reactions can be significantly affected by solvent polarity even in the absence of conformational changes,³⁴ β -isoquinidine (β -iQD), which only adopts open conformations, was exploited to account for such types of solvent effects.^{40a} By comparing the relative rate constant of the reaction with QD ($k_{QD}/k_{\beta iQD}$) in different solvents, the role of conformations in reaction kinetics can be inferred. Figure 8B shows a plot of $k_{QD}/k_{\beta iQD}$ as a function of the population of open conformations of QD (Pop_{open}) in various solvents. Although the relationship is not linear, a noticeable trend can be seen as the relative reaction rate constant, $k_{QD}/k_{\beta iQD}$, increases with the increase of Pop_{open} (see SI for details). In line with the notably higher reaction rate constant with β -iQD than that with QD, the observed trend implies that the open conformations are likely to be more reactive than the closed conformations, which presumably can be attributed to the reduced steric hindrance around the reactive quinuclidine-N atom in open conformations.^{40b}

5. CONCLUSIONS

By incorporating a trifluoromethyl group in the C9 carbon of quinidine, the conformational exchange can be significantly decelerated to allow the direct determination of the conformational distribution in various solvents. With these results, the reliability of the PCM model-based theoretical calculation was assessed, which demonstrated considerable divergence from the experimental data. These errors in theoretical calculations are mainly due to the complicated solvent–cinchona alkaloids interaction mechanism that cannot be fully described by the PCM model. In fact, only the conformers with calculated Gibbs free energies higher than 3.5 kcal/mol in the gas phase can be excluded as populated species in solution. Based on the present results and Baiker's seminal two-equation, two-variable linear system, the open–closed conformational equilibria in various solvents were determined. It was found that the previous correlation of the open-3 population of cinchona alkaloids with the dielectric constant of solvents was in fact unsuccessful. Instead, the LFER analysis using multiparameter polarity scales has been proven to be a powerful tool for quantitative prediction of solvent effects on the conformational behavior of cinchona alkaloids and their derivatives. The importance of solvent-induced conformational distributions was demonstrated in a case study of the S_N2 reaction between QD and α -bromoacetate, which suggests a higher reactivity of open conformations compared to closed conformations. Overall, the current result reveals a complicated solvent–solute interaction scenario involving both nonspecific and specific forces.

■ ASSOCIATED CONTENT

Supporting Information

Experimental procedures, calculation details, analytical data, and NMR spectra. This material is available free of charge via the Internet at <http://pubs.acs.org>.

■ AUTHOR INFORMATION

Corresponding Author

gprakash@usc.edu

Notes

The authors declare no competing financial interest.

ACKNOWLEDGMENTS

Financial support for our work by the Loker Hydrocarbon Research Institute is greatly acknowledged. Prof. T. Williams is gratefully thanked for his valuable suggestions and discussions on the manuscript. The computational studies were supported by the University of Southern California Center for High-Performance Computing and Communications. Mr. J.-P. Jones is acknowledged for providing additional computational resources.

REFERENCES

- (1) (a) Kolb, H. C.; VanNieuwenhze, M. S.; Sharpless, K. B. *Chem. Rev.* **1994**, *94*, 2483–2547. (b) O'Donnell, M. J. *Acc. Chem. Res.* **2004**, *37*, 506–517. (c) Chen, Y.; McDaid, P.; Deng, L. *Chem. Rev.* **2003**, *103*, 2965–2983. (d) France, S.; Guerin, D. J.; Miller, S. J.; Lectka, T. *Chem. Rev.* **2003**, *103*, 2985–3012. (e) Yoon, T. P.; Jacobsen, E. N. *Science* **2003**, *299*, 1691–1693. (f) Song, C. E., Ed. *Cinchona Alkaloids in Synthesis and Catalysis*; Wiley-VCH: Weinheim, 2009.
- (2) For discussions on conformational effects on chemical reactivity, see: Seeman, J. I. *Chem. Rev.* **1983**, *83*, 84–134.
- (3) (a) Hiemstra, H.; Wynberg, H. *J. Am. Chem. Soc.* **1981**, *103*, 417–430. (b) Dijkstra, G. D. H.; Kellogg, R. M.; Wynberg, H.; Svendsen, J. S.; Marko, I.; Sharpless, K. B. *J. Am. Chem. Soc.* **1989**, *111*, 8069–8076. (c) Svendsen, J. S.; Markó, I. E.; Jacobsen, E. N.; Pulla Rao, C.; Bott, S.; Sharpless, K. B. *J. Org. Chem.* **1989**, *54*, 2263–2264.
- (4) (a) Corey, E. J.; Noe, M. C. *J. Am. Chem. Soc.* **1993**, *115*, 12579–12580. (b) Corey, E. J.; Noe, M. C.; Sarshar, S. *Tetrahedron Lett.* **1994**, *35*, 2861–2864. (c) Corey, E. J.; Noe, M. C. *J. Am. Chem. Soc.* **1996**, *118*, 319–329. (d) Li, H.; Liu, X.; Wu, F.; Tang, L.; Deng, L. *Proc. Natl. Acad. Sci. U.S.A.* **2010**, *107*, 20625–20629.
- (5) Bürgi, T.; Baiker, A. *J. Am. Chem. Soc.* **1998**, *120*, 12920–12926.
- (6) (a) Bucher, C.; Mondelli, C.; Baiker, A.; Gilmour, R. *J. Mol. Catal. A: Chem.* **2010**, *327*, 87–91. (b) Zimmer, L. E.; Sparr, C.; Gilmour, R. *Angew. Chem., Int. Ed.* **2011**, *50*, 11860–11871. (c) Schmidt, E.; Bucher, C.; Santarossa, G.; Mallat, T.; Gilmour, R.; Baiker, A. *J. Catal.* **2012**, *289*, 238–248. (d) Tanzer, E.-M.; Schweizer, W. B.; Ebert, M.-O.; Gilmour, R. *Chem.—Eur. J.* **2012**, *18*, 2006–2013.
- (7) (a) Aune, M.; Matsson, O. *J. Org. Chem.* **1995**, *60*, 1356–1364. (b) Busygin, I.; Nieminen, V.; Taskinen, A.; Sinkkonen, J.; Toukoniitty, E.; Sillanpää, R.; Murzin, D. Yu.; Leino, R. *J. Org. Chem.* **2008**, *73*, 6559–6569.
- (8) (a) Vayner, G.; Houk, K. N.; Sun, Y.-K. *J. Am. Chem. Soc.* **2004**, *126*, 199–203 and references therein. (b) Vargas, A.; Bürgi, T.; Baiker, A. *J. Catal.* **2004**, *226*, 69–82. (c) Çelebi-Ölçüm, N.; Aviyente, V.; Houk, K. N. *J. Org. Chem.* **2009**, *74*, 6944–6952.
- (9) (a) Ferri, D.; Bürgi, T.; Baiker, A. *J. Chem. Soc., Perkin Trans. 2* **1999**, 1305–1311. (b) Ferri, D.; Bürgi, T.; Borszaky, K.; Mallat, T.; Baiker, A. *J. Catal.* **2000**, *193*, 139–144. (c) Meier, D. M.; Urakawa, A.; Turrà, N.; Rüegger, H.; Baiker, A. *J. Phys. Chem. A* **2008**, *112*, 6150–6158. (d) Urakawa, A.; Meier, D. M.; Rüegger, H.; Baiker, A. *J. Phys. Chem. A* **2008**, *112*, 7250–7255. (e) Bürgi, T.; Vargas, A.; Baiker, A. *J. Chem. Soc., Perkin Trans. 2* **2002**, *9*, 1596–1601.
- (10) Olsen, R. A.; Borchardt, D.; Mink, L.; Agarwal, A.; Mueller, L. J.; Zaera, F. *J. Am. Chem. Soc.* **2006**, *128*, 15594–15595.
- (11) Karle, J. M.; Bhattacharjee, A. K. *Bioorg. Med. Chem.* **1999**, *7*, 1769–1774.
- (12) (a) Prelog, V.; Wilhelm, M. *Helv. Chim. Acta* **1954**, *37*, 1634–1660. (b) Dijkstra, G. D. H.; Kellogg, R. M.; Wynberg, H. *J. Org. Chem.* **1990**, *55*, 6121–6131.
- (13) For recent discussion on PCM models, see: Mennucci, B. *J. Phys. Chem. Lett.* **2010**, *1*, 1666–1674.
- (14) Karplus, M. *J. Chem. Phys.* **1959**, *30*, 11–15.
- (15) Neuhaus, D.; Williamson, M. P. *The Nuclear Overhauser Effect in Structural and Conformational Analysis*, 2nd ed.; John Wiley & Sons: New York, 2000; pp 321–322 and 391–398.
- (16) For discussions on steric effects of the trifluoromethyl group, see: (a) Schlosser, M.; Michel, D. *Tetrahedron* **1996**, *52*, 99–108. (b) Uneyama, K. *Organofluorine Chemistry*; Blackwell: Oxford, 2006; pp 82–83. (c) Charton, M. *J. Am. Chem. Soc.* **1975**, *97*, 1552–1556.
- (17) (a) Prakash, G. K. S.; Wang, F.; Ni, C.; Shen, J.; Haiges, R.; Yudin, A. K.; Mathew, T.; Olah, G. A. *J. Am. Chem. Soc.* **2011**, *133*, 9992–9995. (b) Prakash, G. K. S.; Wang, F.; Rahm, M.; Shen, J.; Ni, C.; Haiges, R.; Olah, G. A. *Angew. Chem., Int. Ed.* **2011**, *50*, 11761–11764.
- (18) For a comprehensive book describing ^{19}F NMR spectroscopy, see: Dolbier, W. R., Jr. *Guide to Fluorine NMR for Organic Chemists*; John Wiley and Sons: Hoboken, NJ, 2009; pp 4–5.
- (19) Frisch, M. J.; Trucks, G. W.; Schlegel, H. B.; Scuseria, G. E.; Robb, M. A.; Cheeseman, J. R.; Scalmani, G.; Barone, V.; Mennucci, B.; Petersson, G. A.; Nakatsuji, H.; Caricato, M.; Li, X.; Hratchian, H. P.; Izmaylov, A. F.; Bloino, J.; Zheng, G.; Sonnenberg, J. L.; Hada, M.; Ehara, M.; Toyota, K.; Fukuda, R.; Hasegawa, J.; Ishida, M.; Nakajima, T.; Honda, Y.; Kitao, O.; Nakai, H.; Vreven, T.; Montgomery, J. A., Jr.; Peralta, J. E.; Ogliaro, F.; Bearpark, M.; Heyd, J. J.; Brothers, E.; Kudin, K. N.; Staroverov, V. N.; Kobayashi, R.; Normand, J.; Raghavachari, K.; Rendell, A.; Burant, J. C.; Iyengar, S. S.; Tomasi, J.; Cossi, M.; Rega, N.; Millam, N. J.; Klene, M.; Knox, J. E.; Cross, J. B.; Bakken, V.; Adamo, C.; Jaramillo, J.; Gomperts, R.; Stratmann, R. E.; Yazyev, O.; Austin, A. J.; Cammi, R.; Pomelli, C.; Ochterski, J. W.; Martin, R. L.; Morokuma, K.; Zakrzewski, V. G.; Voth, G. A.; Salvador, P.; Dannenberg, J. J.; Dapprich, S.; Daniels, A. D.; Farkas, Ö.; Foresman, J. B.; Ortiz, J. V.; Cioslowski, J.; Fox, D. J. *Gaussian 09*, Revision B.01; Gaussian, Inc., Wallingford CT, 2009.
- (20) This computational approach was previously validated as a feasible estimation to the energetic and geometric properties of conformations with satisfactory accuracy: Hamza, A.; Schubert, G.; Soós, T.; Papai, I. *J. Am. Chem. Soc.* **2006**, *128*, 13151.
- (21) Zhao, Y.; Truhlar, D. G. *Theor. Chem. Acc.* **2008**, *120*, 215–241.
- (22) (a) Miertuš, S.; Scrocco, E.; Tomasi, J. *J. Chem. Phys.* **1981**, *55*, 117–129. (b) Scalmani, G.; Frisch, M. J. *J. Chem. Phys.* **2010**, *132*, 114110.
- (23) In this article, PCM is used as a synonym for IEFPCM.
- (24) (a) Reed, A. E.; Curtiss, L. A.; Weinhold, F. *Chem. Rev.* **1988**, *88*, 899–926. (b) Glendening, E. D.; Reed, A. E.; Carpenter, J. E.; Weinhold, F. *NBO*, Version 3.1, 1996.
- (25) For recent applications of LFER in mechanistic studies, see: (a) Jensen, K. H.; Sigman, M. S. *Angew. Chem., Int. Ed.* **2007**, *46*, 4748–4750. (b) Baidya, M.; Kobayashi, S.; Brotzel, F.; Schmidhammer, U.; Riedle, E.; Mayr, H. *Angew. Chem., Int. Ed.* **2007**, *46*, 6176–6179. (c) Sigman, M. S.; Miller, J. J. *J. Org. Chem.* **2009**, *74*, 7633–7643. (d) Knowles, R. R.; Lin, S.; Jacobsen, E. N. *J. Am. Chem. Soc.* **2010**, *132*, 5030–5032. (e) Jensen, K. H.; Sigman, M. S. *J. Org. Chem.* **2010**, *75*, 7194–7201. (f) Li, X.; Deng, H.; Zhang, B.; Li, J.; Zhang, L.; Luo, Z.; Cheng, J.-P. *Chem.—Eur. J.* **2010**, *16*, 450–455. (g) Harper, K. C.; Sigman, M. S. *Proc. Natl. Acad. Sci. U.S.A.* **2011**, *108*, 2179–2183. (h) Harper, K. C.; Sigman, M. S. *Science* **2011**, *333*, 1875–1878. (i) Harper, K. C.; Bess, E. N.; Sigman, M. S. *Nat. Chem.* **2012**, *4*, 366–374. (j) Gormisky, P. E.; White, M. C. *J. Am. Chem. Soc.* **2013**, *135*, 14052–14055. (k) Prakash, G. K. S.; Zhang, Z.; Wang, F.; Rahm, M.; Ni, C.; Iulicci, M.; Haiges, R.; Olah, G. A. *Chem.—Eur. J.* **2014**, *20*, 831–838.
- (26) (a) Wells, P. R. *Chem. Rev.* **1963**, *63*, 171–219. (b) Koppel, I. A.; Palm, V. A. *Advances in Linear Free Energy Relationships*; Chapman, N. B.; Shorter, J., Eds.; Plenum Press: London, 1972; pp 203–280.
- (27) (a) Reichardt, C. *Angew. Chem., Int. Ed. Engl.* **1979**, *18*, 98–110. (b) Reichardt, C.; Welton, T. *Solvents and Solvent Effects in Organic Chemistry*, 4th ed.; Wiley-VCH: Weinheim, 2011.
- (28) Onsager, L. *J. Am. Chem. Soc.* **1936**, *58*, 1486–1493.
- (29) Approximate linear relationships have been found between various dielectric functions, including $1/\epsilon$, $(\epsilon - 1)/(\epsilon + 1)$, $(\epsilon - 1)/(\epsilon + 2)$, and $(\epsilon - 1)/(2\epsilon + 1)$. For example, $(\epsilon - 1)/(\epsilon + 2)$ and $(\epsilon - 1)/(2\epsilon + 1)$ have correlation coefficients (R^2) of 0.978 and 0.991 when $\epsilon \geq 1$ and 3, respectively. Therefore, these dielectric functions are practically interchangeable. See ref 27b, pp 215–216.

(30) $\Delta G_{\text{open-3,exp}}$ of cinchonidine in various solvents was calculated on the basis of the reported population ratio of open-3 conformation and closed conformations ($\text{Pop}_{\text{open-3,exp}}/\text{Pop}_{\text{closed,exp}}$).

(31) Selected reviews on multiparameter solvation models: (a) Katritzky, A. R.; Fara, D. C.; Yang, H.; Tamm, K. *Chem. Rev.* **2004**, *104*, 175–198. (b) Marcus, Y. *Chem. Soc. Rev.* **1993**, *22*, 409–416.

(32) Kamlet, M. J.; Abboud, J.-L. M.; Abraham, M. H.; Taft, R. W. J. *Org. Chem.* **1983**, *48*, 2877–2887.

(33) (a) Abboud, J. L.; Kamlet, M. J.; Taft, R. W. J. *Am. Chem. Soc.* **1977**, *99*, 8325–8327. (b) Laurence, C.; Nicolet, P.; Dalati, M. T.; Abboud, J. L. M.; Notario, R. J. *Phys. Chem.* **1994**, *98*, 5807–5816.

(34) Using original Kamlet–Taft solvent polarity expression ($XYZ = XYZ_0 + a \cdot \alpha + b \cdot \beta + s \cdot \pi + d \cdot \delta$), $\Delta G_{\text{open,exp}}$ is correlated to multipolarity with $R^2 = 0.705$. δ is a discontinuous polarizability correction term, equal to 1.0, 0.5, and 0.0 for aromatic, polychlorinated, and all other aliphatic solvents, respectively. δ possibly oversimplified the solvent effects. Reichardt, C.; Welton, T. *Solvents and Solvent Effects in Organic Chemistry*, 4th ed.; Wiley-VCH: Weinheim, 2011; p 497. In the present study, continuous polarizability P , $(n^2 - 1)/(n^2 + 1)$, was found to be a better correction term.

(35) Reichardt, C. *Chem. Rev.* **1994**, *94*, 2319–2358.

(36) Haasnoot, C. A. G.; DeLeeuw, F. A. A. M.; Altona, C. *Tetrahedron* **1980**, *36*, 2783–2792.

(37) Cinchona alkaloids are known to form π – π complexes at high concentrations in solution: (a) Uccello-Barretta, G.; Bari, L. D.; Salvadori, P. *Magn. Reson. Chem.* **1992**, *30*, 1054–1063. (b) Marchettini, N.; Valensin, G.; Gaggelli, E. J. *Phys. Chem. A* **2004**, *108*, 8505–8513.

(38) (a) Papageorgiou, C. D.; Ley, S. V.; Gaunt, M. J. *Angew. Chem., Int. Ed.* **2003**, *42*, 828–831. (b) Bremeyer, N.; Smith, S. C.; Ley, S. V.; Gaunt, M. J. *Angew. Chem., Int. Ed.* **2004**, *43*, 2681–2684. (c) Papageorgiou, C. D.; Cubilos de Dios, M. A.; Ley, S. V.; Gaunt, M. J. *Angew. Chem., Int. Ed.* **2004**, *43*, 4641–4644. (d) Johansson, C. C.; Bremeyer, N.; Ley, S. V.; Owen, D. R.; Smith, S. C.; Gaunt, M. J. *Angew. Chem., Int. Ed.* **2006**, *45*, 6024–6028. (e) A detailed mechanistic investigation on catalytically active conformations of cinchona alkaloid derivatives in Gaunt's cyclopropanation will be reported in due course.

(39) Waldmann, H.; Khedkar, V.; Dücker, H.; Markus Schürmann, M.; Oppel, I. M.; Kumar, K. *Angew. Chem., Int. Ed.* **2008**, *47*, 6869–6872.

(40) (a) Solvent effects in the S_N2 reaction of simple trialkylamine with alkyl halides: Abraham, M. H. *J. Chem. Soc. B* **1971**, 299–308. (b) Our calculations at the PCM-M06-2X/6-311+G(d,p)//PCM-B3LYP/6-311+G(d,p) level of theory revealed that the barrier to the reaction between the closed-2 conformation of *O*-methylated quinidine (MeOQD) and α -bromoacetate in MeCN is ca. 2.0 kcal/mol higher than that of the open-3 conformation. These results are in good agreement with the current kinetic experiments and will be reported along with the study mentioned in ref 38e.